

Soft X-ray resonant scattering study of single-crystal $\text{LaSr}_2\text{Mn}_2\text{O}_7$

H.-F. Li^{1,4}, Y. Su¹, Tapan Chatterji^{1,2}, A. Nefedov³, J. Persson¹, P. Meuffels¹, Y. Xiao¹, and Th. Brückel¹

¹*Institut für Festkörperforschung, Forschungszentrum Jülich GmbH, D-52425 Jülich, Germany*

²*Institut Laue-Langevin, BP 156, F-38042 Grenoble Cedex 9, France*

³*Institut für Experimentalphysik/Festkörperphysik, Ruhr-Universität Bochum, Germany*

⁴*Ames Laboratory and Department of Physics and Astronomy, Iowa State University, Ames, Iowa 50011, USA*

(Dated: July 2, 2021)

Soft X-ray resonant scattering studies at the Mn L_{II} , III - and the La M_{IV} , ν - edges of single-crystal $\text{LaSr}_2\text{Mn}_2\text{O}_7$ are reported. At low temperatures, below $T_{\text{N}} \approx 160$ K, energy scans with a fixed momentum transfer at the A -type antiferromagnetic $(0\ 0\ 1)$ reflection around the Mn L_{II} , III -edges with incident linear σ and π polarizations show strong resonant enhancements. The splitting of the energy spectra around the Mn L_{II} , III -edges may indicate the presence of a mixed valence state, e.g., $\text{Mn}^{3+}/\text{Mn}^{4+}$. The relative intensities of the resonance and the clear shoulder-feature as well as the strong incident σ and π polarization dependences strongly indicate its complex electronic origin. Unexpected enhancement of the charge Bragg $(0\ 0\ 2)$ reflection at the La M_{IV} , ν -edges with σ polarization has been observed up to 300 K, with an anomaly appearing around the orbital-ordering transition temperature, $T_{\text{OO}} \approx 220$ K, suggesting a strong coupling (competition) between them.

PACS numbers: 61.10.-i, 71.30.+h, 75.25+z, 75.47.Lx

INTRODUCTION

Strongly correlated electron systems such as $3d$ transition-metal (TM) oxides present exciting fundamental properties, e.g., the superconducting behavior or the extraordinary colossal magnetoresistance effect. Their rich structural, magnetic and electronic properties are governed by the interplay of lattice, spin, charge and orbital degrees of freedom. Identification and precise characterization of the ordered phases is a prerequisite for understanding the physical properties and unusual phenomena. Among all possible experimental techniques, resonant X-ray scattering combined with its spectroscopic characteristics stands out due to its unique sensitivity to probe the charge/orbital ordering (CO/OO). With the application of resonant X-ray scattering in the hard X-ray regime [1], significant progress on the experimental quest of the orbital degree of freedom in $3d$ TM compounds has been made. The resonant enhancement of the CO/OO super-reflections in $\text{LaSr}_2\text{Mn}_2\text{O}_7$ has been observed at the Mn K -edge [2, 3]. However, the resonance at the K -edge of $3d$ TMs is due to dipolar excitations from the $1s$ to $4p$ band and thus only indirectly reflects the $3d$ electronic states. An alternative way is the resonant soft X-ray scattering. This is a powerful technique for directly probing the ordered phases individually. Utilizing this method, some studies [4–6] show strong resonant enhancements of the expected superlattice reflections around the Mn L_{II} , III -edges ($2p \rightarrow 3d$) which are known to be very sensitive to the details of the $3d$ electronic states, supporting direct and definitive evidences for the ordering of charge, orbital and spin degrees of freedom in various manganites.

The compounds $\text{La}_{2-2x}\text{Sr}_{1+2x}\text{Mn}_2\text{O}_7$ consist of MnO_2 bilayers separated by the rock-salt-type $(\text{La}, \text{Sr})_2\text{O}_2$ blocking bilayers. They are stacked vertically along the

c axis ($I4/mmm, Z = 2$) as shown in Fig. 1(a) taking the half-doped $\text{LaSr}_2\text{Mn}_2\text{O}_7$ ($x = 0.5$) as an example. Though no structural transition was reported for $\text{LaSr}_2\text{Mn}_2\text{O}_7$ below room temperature [7], this compound undergoes a transition into the CE -type charge-orbital ordered state at ~ 225 K [2]. This state starts melting around 170 K where the A -type antiferromagnetic (A -AFM) structure forms [Fig. 1(a)]. The $(0\ 0\ 1)$ reflection corresponds to this long-range A -AFM ordering stacked along the crystallographic c axis. The CO/OO breaks down at ~ 100 K but recovers again around 50 K. This reentrant behavior was discussed in terms of a polaron model [2]. In addition, the minor CE -AFM phase was reported to coexist with the major A -AFM one below ~ 145 K and be drastically but not completely suppressed below ~ 100 K. This phenomenon was viewed as an effective phase separation [8].

In this article, we report a resonant soft X-ray scattering study of the AFM $(0\ 0\ 1)$ and the charge Bragg $(0\ 0\ 2)$ reflections in $\text{LaSr}_2\text{Mn}_2\text{O}_7$, varying incident photon polarizations. The detailed energy and temperature dependencies were monitored. Our study confirms that the energy spectra of the AFM $(0\ 0\ 1)$ over the Mn L_{II} , III -edges consist of six clear features. In addition, we found a huge resonant enhancement of the charge Bragg $(0\ 0\ 2)$ reflection at the La M_{IV} , ν -edges.

EXPERIMENTAL DETAILS

Most available soft X-ray scattering chambers host two-circle diffractometers. This geometry leads to severe restrictions for sample rotating around the surface normal (ψ -circle) and sample tilting (χ -circle) [Fig. 2(a)], which are both essential degrees of freedom for single-crystal resonant soft X-ray scattering studies. Therefore,

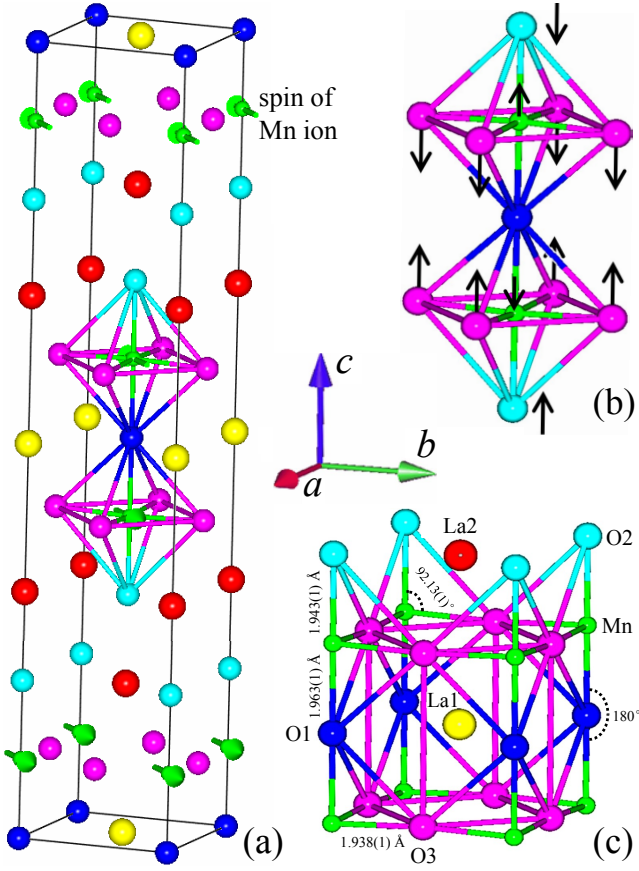


FIG. 1: (color online) (a) Structural ($I4/mmm$, $Z = 2$) unit-cell of $\text{LaSr}_2\text{Mn}_2\text{O}_7$ and arrangement of A -AFM spins of Mn ions. Structural parameters were taken from [7]. (b) An octahedron of MnO_6 along the c axis and its distortion mode. (c) Local crystal environments for the La1 and La2 sites.

a precise pre-alignment on the sample to be measured is crucial. Even when such a perfect pre-alignment is possible, any small angular deviations that often appear during the cooling of the sample or due to the temperature-dependent change of the lattice parameters may still easily ruin the efforts. To overcome these limitations, a new portable ultrahigh-vacuum (UHV) goniometer has been designed and built for resonant soft X-ray scattering, which makes it feasible to adjust samples along χ ($\pm 2.5^\circ$) and ψ (360°). This miniature goniometer dramatically improves the efficiency of soft X-ray scattering chambers. Single crystals of $\text{LaSr}_2\text{Mn}_2\text{O}_7$ were grown by the floating-zone method [9]. A polished one was mounted on the center of a copper plate braced to the goniometer (Fig. 2) with $[0\ 0\ 1]$ direction nearly normal to the scattering plane. Resonant soft X-ray scattering data were collected on the two-circle UHV ALICE diffractometer [10] equipped with our goniometer at the UE56/1-PGM-b beamline of the BESSY, Germany. The vertical scattering geometry is shown in Fig. 2(b) where ψ is the so-called azimuthal angle which represents the

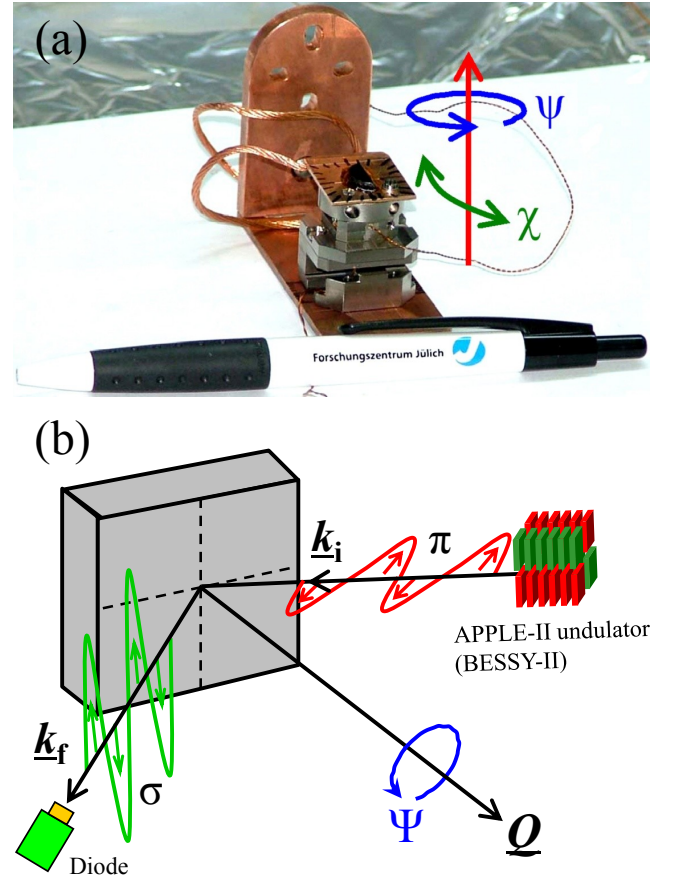


FIG. 2: (color online) (a) Miniature goniometer utilized in this study for rotating and tilting the $\text{LaSr}_2\text{Mn}_2\text{O}_7$ sample in ψ and χ angles, respectively. (b) Basic notations for the resonant soft X-ray scattering set-up at the UHV ALICE diffractometer at Berliner Elektronen-Speicherring Gesellschaft für Synchrotronstrahlung (BESSY).

relative orientation of the sample with respect to \mathbf{Q} .

RESULTS AND DISCUSSION

Fig. 3(a) shows the energy dependence of the integrated intensity of the AFM $(0\ 0\ 1)$ through the Mn L_{II} , L_{III} -edges at 15 K. A similar observation on this compound was previously reported [11] where only observed intensity without polarization analysis was recorded at 20 K. Clearly, the present study is more detailed. The spectra show a very strong polarization dependence and are dominated by scattering at the Mn L_{III} -edge. Six clear features are present: four peaks (2, 4, 5 and 6) and two shoulders (1 and 3). The intensity ratio between the two main features 2 and 4 is reversed with the different polarizations. The splitting of the energy spectra with σ and π polarizations around the Mn L_{II} , L_{III} -edges is probably ascribed to the existence of a mixed valence state, e.g., $\text{Mn}^{3+}/\text{Mn}^{4+}$ type. The contrast intensity between both

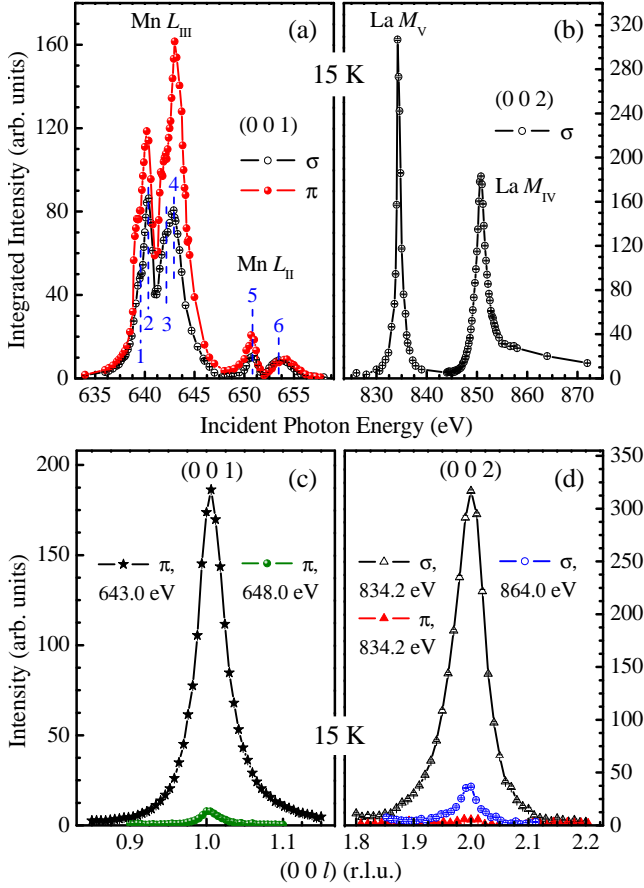


FIG. 3: (color online) Energy dependence of (a) AFM (0 0 1) recorded over the Mn L_{II} , L_{III} -edges and (b) charge Bragg (0 0 2) reflection over the La M_{IV} , M_V -edges with incident linear σ and π polarizations at 15 K. The intensity was integrated from longitudinal scans at each energy point. (c) and (d) longitudinal scans of the (0 0 1) and (0 0 2) reflections, respectively, at and off their strongest resonant energies ~ 643.0 eV (Mn L_{III} -edge) and ~ 834.2 eV (La M_V -edge).

spectra results from different orientations of the incident linear σ and π X-ray relative to the magnetic moments. The resonance of the charge Bragg (0 0 2) reflection at the La M_{IV} , M_V -edges with σ polarization [(Fig. 3(b)] was unexpectedly observed at 15 K. This resonant enhancement is extremely large and has dramatic polarization dependence at the La M_{IV} , M_V -edges as shown in Fig. 3(d) where the resonance with the incident π polarization is very small. Figures. 3(c) and (d) comparatively show the longitudinal scans of the AFM (0 0 1) and the charge Bragg (0 0 2) reflections, respectively, at and off their strongest resonant energies ~ 643.0 eV (Mn L_{III} -edge) and ~ 834.2 eV (La M_V -edge).

The temperature dependences of the AFM (0 0 1) reflection at the six energies corresponding to the six features 1, 2, 3, 4, 5 and 6 [Fig. 3(a)] and the charge Bragg (0 0 2) reflection at the La M_V -edge with σ polarization upon warming were shown in Fig. 4. The integrated

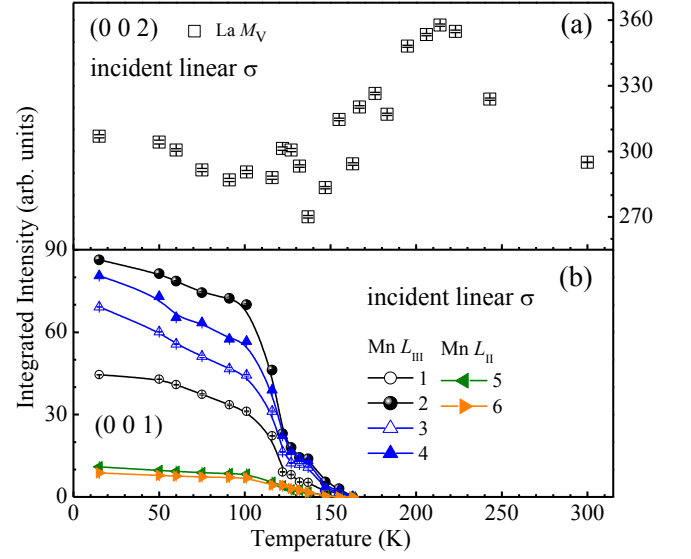


FIG. 4: (color online) Temperature dependent integrated intensity (measured in the longitudinal direction) of (a) charge Bragg (0 0 2) reflection at the La M_V -edges, and (b) AFM (0 0 1) reflection recorded at the six energies corresponding to the six features 1, 2, 3, 4, 5 and 6 as labeled in Fig. 3(a).

intensities of the AFM (0 0 1) decrease gradually as increasing temperature to $T_N \sim 160$ K and then disappear simultaneously [Fig. 4(b)]. The intensity of the charge Bragg (0 0 2) reflection persists up to 300 K and exhibits a broad peak around 220 K [Fig. 4(a)]. The recorded intensity of the charge Bragg (0 0 2) reflection over the Mn L_{II} , L_{III} - and the La M_{IV} , M_V - edges at 300 K was shown in Fig. 5(a). The corresponding longitudinal scans at the Mn L_{II} - and the La M_V - edges were shown in Fig. 5(b). The intensity ratio between the two main peaks at the Mn L_{III} -edge keeps the numerical relationship with σ and π polarizations. Compared to Ref. [4] where the $\text{La}_{1.05}\text{Sr}_{1.95}\text{Mn}_2\text{O}_7$ sample was investigated, the resonance observed here has a different spectral shape and much clearer features, i.e., an obvious peak splitting at the Mn L_{III} -edge, probably ascribing to the different Mn 3d electronic states and the different scattering factors of the charge Bragg (0 0 2) reflection resulting from the different doping levels. Whereas, the spectra around the La M_{IV} , M_V -edges involve only a single resonant peak each and this resonant enhancement is extremely large with dramatic polarization dependence as shown in Fig. 5. Developing a correct theoretical model to simulate the observed energy spectra is indispensable for further understanding the physics behind.

Superlattice reflections corresponding to the propagation vector $\mathbf{Q} = (\frac{1}{4}\frac{1}{4}0)$ in $\text{LaSr}_2\text{Mn}_2\text{O}_7$ were believed to be relevant to the 3d OO ($3x^2 - r^2/3y^2 - r^2$) of Mn^{3+} ions, which is accompanied by the CO of 1:1 $\text{Mn}^{3+}/\text{Mn}^{4+}$ species [12]. X-ray, neutron and electron diffraction studies [2, 12] indicate that the coupled CO/OO developed

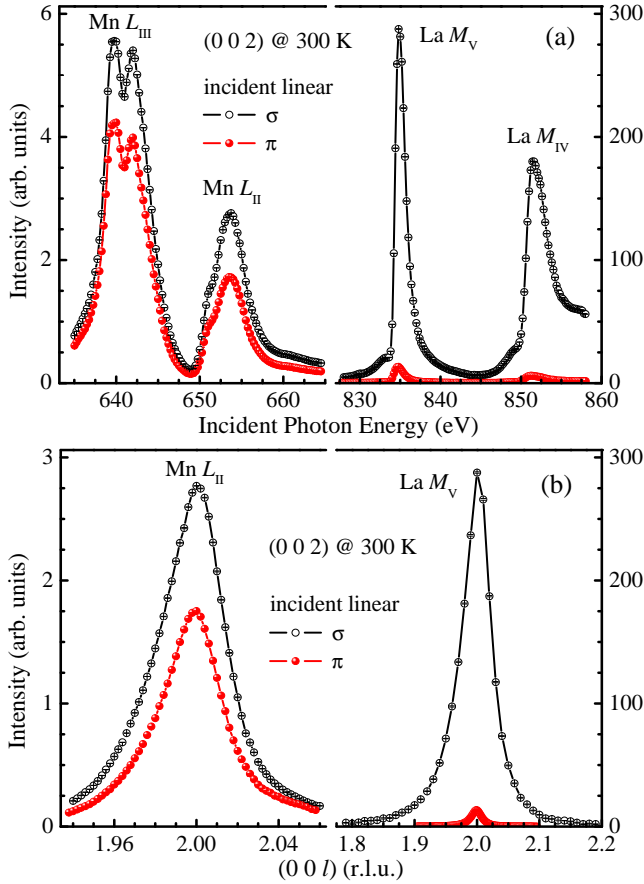


FIG. 5: (color online) (a) Energy dependence of charge Bragg (0 0 2) reflection recorded over the Mn L_{II} , L_{III} - (left) and the La M_{IV} , v - (right) edges at constant wavevector with incident linear σ and π polarizations at 300 K. (b) Corresponding longitudinal scans at the Mn L_{II} - and the La M_V - edges.

at ~ 225 K starts melting at the A -AFM transition temperature, ~ 170 K, and collapses below ~ 100 K. However, the CO wavevector was subsequently suggested to be $(\frac{1}{2}\frac{1}{2}0)$ different with that of the OO [3]. The direct observation of the orbital reflection $(\frac{1}{4}\frac{1}{4}0)$ [11] using resonant soft X-ray scattering technique at the Mn L_{II} , L_{III} -edges shows that the OO develops at ~ 225 K and persists down to ~ 20 K, with a small change in the gradient of the observed intensity below ~ 100 K. Comparing Refs. [3, 11, 12], it seems that the OO causes an occurrence of the CO and subsequently drives the formation of the long-range A -AFM spin ordering. The breakdown of CO is due to the ferromagnetic spin couplings in crystallographic a - b plane in the AFM state. In addition, the change in the temperature-dependent integrated intensity of the charge Bragg (0 0 2) reflection at the La M_V -edges [Fig. 4(a)] seems to be inversely correlated to that of the OO reported in [11], indicating a possible competition between them. Therefore, complicated cooperation and competition between spin, charge, orbital and lattice degrees of freedom exist in double-layered $\text{LaSr}_2\text{Mn}_2\text{O}_7$.

It is interesting to explore the reasons for the huge resonant enhancement of the charge Bragg (0 0 2) reflection at the La M_{IV} , v -edges. This peak is allowed for the tetragonal structure of this compound. The observed intensity in resonant soft X-ray scattering is mainly determined by the anomalous atomic scattering factor of the resonant atoms. This factor is a function of the incident photon energy E and can be expressed as $f(E) = f_1(E) + if_2(E)$, where the imaginary part $f_2(E)$ is related to the absorption coefficient and the real part $f_1(E)$ can be deduced from $f_2(E)$ through the mutual Kramers-Kronig relation [13]. The X-ray absorption spectrum of this compound at the La M_{IV} , v -edges needs to be measured for a quantitative calculation of the anomalous scattering factor. The anomalous atomic scattering factor shows a tensorial character and its anisotropy is mainly related to the distortion of the local environment. During the resonant soft X-ray scattering process, in principle, the excited electron is sensitive to any anisotropy around the absorbing ions, e.g., the anisotropy of charge, orbital, spin or lattice. There are two types of distortion related to the MnO_6 octahedra in manganites: (i) one is the Jahn-Teller (JT) distortion that is inherent to the high-spin ($S = 2$) Mn^{3+} ions, resulting in different Mn-O bond lengths, which is accompanied by the OO of occupied Mn $3d$ orbitals; (ii) another is the cooperative rotation corresponding to the Mn-O-Mn bond angle and tolerance factor, leading to lattice modulations and forming the octahedral tilt-ordering (TO). An octahedral TO of $\text{Pr}_{1-x}\text{Ca}_x\text{MnO}_3$ and LaMnO_3 [14] was observed by tuning the incident X-ray energy to the L_I , L_{II} , and L_{III} absorption edges of Pr and La, respectively. The structural data of $\text{LaSr}_2\text{Mn}_2\text{O}_7$ as a function of temperature was not completed [15] and the existing structural parameters were strongly challenged by the single-crystal study [16]. The tetragonal symmetry ($I4/mmm$) of $\text{LaSr}_2\text{Mn}_2\text{O}_7$ determines that the out-of-plane Mn-O-Mn bond angle along the c axis is 180° and the JT distortion size which is defined as the ratio of the averaged apical and the equatorial Mn-O bond lengths is close to unity down to 10 K [Fig. 1(c)]. Thus no octahedral TO exists in $\text{LaSr}_2\text{Mn}_2\text{O}_7$. However, the distortion mode developed for the MnO_6 octahedra based on the Mn-O bond lengths indeed exists [Fig. 1(b)], which was confirmed by a Raman spectroscopy study [17]. Raman spectroscopy is a very sensitive probe of the local and dynamical structural changes. This scattering method can be used to study the complex interplay of lattice dynamics with ordering parameters in manganites. In [17], the major intensity of out-of-plane spectra was assigned to this stretching mode [Fig. 1(b)] and is independent of temperature. In addition, two tiny intensities in out-of-plane spectra were attributed to the Raman allowed modes in the original structure: atomic motion of La/Sr ions along the c direction. Moreover, the rest appreciable intensities were thought to be from the

activated modes, i.e., the coupling between lattice distortion and CO/OO. This octahedral distortion mode has little effect on the local crystal environment of La1 sites that locate at the center of four double-MnO₆ octahedra [Fig. 1(c)], while it has a profound effect on that of the La2 sites due to the asymmetric action. Indeed, based on the reported structural parameters at room temperature [7], the calculated local distortion sizes of La1 and La2 sites by Fullprof suite [18] are 3.2×10^{-5} and 1.4×10^{-3} , respectively. The strongly produced anisotropy of La2 sites may lead to the resonant enhancement of the charge Bragg (0 0 2) reflection at the La M_{IV} , v -edges. In addition, the observed competition between OO and temperature dependent integrated intensity of the charge Bragg (0 0 2) reflection is in agreement with Ref. [17].

To summarize, a systematic resonant soft X-ray scattering study at the La M_{IV} , v -edges on the possible lattice modulations and at the Mn L_{II} , III -edges on the A-AFM structure in LaSr₂Mn₂O₇ has been accomplished. At 15 K, well below $T_N \sim 160$ K, dramatic enhancements of the charge Bragg (0 0 2) and the AFM (0 0 1) reflections at the La M_{IV} , v - and the Mn L_{II} , III - edges were observed, respectively. The temperature dependences of the AFM (0 0 1) resonance at the six featured energies show a similar trend and disappear simultaneously above T_N . The resonant intensity of the charge Bragg (0 0 2) reflection persists from 15 K to 300 K and was strongly strived by the OO around 220 K.

ACKNOWLEDGMENTS

We are grateful for the excellent technical support from BESSY-II, Germany. This work was partially supported by the BMBF under contract No O3ZA6BC2.

-
- [1] S. Ishihara and S. Maekawa, Rep. Prog. Phys. **65**, 561 (2002).
 - [2] T. Chatterji, G. J. McIntyre, W. Caliebe, R. Suryanarayanan, G. Dhalenne, and A. Revcolevschi, Phys.

- Rev. B **61**, 570 (2000).
- [3] S. B. Wilkins, P. D. Spencer, T. A. W. Beale, P. D. Hatton, M. v. Zimmermann, S. D. Brown, D. Prabhakaran, and A. T. Boothroyd, Phys. Rev. B **67**, 205110 (2003).
- [4] S. B. Wilkins, P. D. Hatton, M. D. Roper, D. Prabhakaran, and A. T. Boothroyd, Phys. Rev. Lett. **90**, 187201 (2003).
- [5] K. J. Thomas, J. P. Hill, S. Grenier, Y.-J. Kim, P. Abbamonte, L. Venema, A. Rusydi, Y. Tomioka, Y. Tokura, D. F. McMorrow, G. Sawatzky, and M. van Veenendaal, Phys. Rev. Lett. **92**, 237204 (2004).
- [6] J. H. Martín, J. García, G. Subías, J. Blasco, M. C. Sánchez, and S. Stanesco, Phys. Rev. B **73**, 224407 (2006).
- [7] M. Kubota, H. Fujioka, K. Hirota, K. Ohoyama, Y. Moritomo, H. Yoshizawa, and Y. Endoh, J. Phys. Soc. Jpn. **69**, 1606 (2000).
- [8] M. Kubota, H. Yoshizawa, Y. Moritomo, H. Fujioka, K. Hirota, and Y. Endoh, J. Phys. Soc. Jpn. **68**, 2202 (1999).
- [9] R. Suryanarayanan, G. Dhalenne, A. Revcolevschi, W. Prellier, J. P. Renard, C. Dupas, W. Caliebe, and T. Chatterji, Solid State Commun. **113**, 267 (2000).
- [10] J. Grabis, A. Nefedov, and H. Zabel, Rev. Sci. Instr. **74**, 4048 (2003).
- [11] S. B. Wilkins, N. Stojić, T. A. W. Beale, N. Binggeli, P. D. Hatton, P. Bencok, S. Stanesco, J. F. Mitchell, P. Abbamonte, and M. Altarelli, J. Phys.: Condens. Matter **18**, L323 (2006).
- [12] T. Kimura, R. Kumai, Y. Tokura, J. Q. Li, and Y. Matsui, Phys. Rev. B **58**, 11081 (1998).
- [13] J. Als-Nielsen and D. McMorrow, Elements of modern X-ray physics (John Wiley and Sons, New York, 2001).
- [14] M. v. Zimmermann, C. S. Nelson, Y.-J. Kim, J. P. Hill, Doon Gibbs, H. Nakao, Y. Wakabayashi, Y. Murakami, Y. Tokura, Y. Tomioka, T. Arima, C.-C. Kao, D. Casa, C. Venkataraman, and Th. Gog, Phys. Rev. B **64**, 064411 (2001).
- [15] C. D. Ling, J. E. Millburn, J. F. Mitchell, D. N. Argyriou, J. Linton, and H. N. Bordallo, Phys. Rev. B **62**, 15096 (2000).
- [16] D. N. Argyriou, H. N. Bordallo, B. J. Campbell, A. K. Cheetham, D. E. Cox, J. S. Gardner, K. Hanif, A. dos Santos, G. F. Strouse, Phys. Rev. B **61**, 15269 (2000).
- [17] K. Yamamoto, T. Kimura, T. Ishikawa, T. Katsufuji, and Y. Tokura, Phys. Rev. B **61**, 14706 (2000).
- [18] J. Rodríguez-Carvajal, Physica B **192**, 55 (1993).